

Weakly Turbulent Pipe Flow of a Power Law Fluid

M. Rudman, H. M. Blackburn, L. J. Graham and L. Pullum

Thermal and Fluid Engineering
 CSIRO BCE, Graham Rd, Highett, Victoria 3091, AUSTRALIA

Abstract

Experiment and simulation of the weakly turbulent flow of a power law fluid in a pipe are presented. The simulation results under-predict the superficial flow velocity by approximately 30% for the cases considered. Velocity profiles also show discrepancy from published results. Despite careful examination of both experimental and numerical methods and results, the cause of the discrepancy is still uncertain. The numerical results suggest that the mean flow profiles approaches the Newtonian profile as the generalised Reynolds number increases.

Introduction

The flow of non-Newtonian fluids in pipes occurs in a wide range of practical applications in the process industries. If the fluid has a significant yield stress, or if its effective viscosity is high, industrially relevant flow rates may occur in the laminar flow regime. However in many cases the flow is turbulent and indeed, there are advantages to operating pipe flows in a transitional flow regime because the specific energy consumption is lowest there and in solids transport, intermittency may be used to keep particles in suspension without the much higher pressure losses of the fully turbulent regime. Although some experimental work has appeared on the transitional and turbulent flow of non-Newtonian fluids, little fundamental understanding exists. General theories of turbulence are lacking for non-Newtonian fluids, and the development of mathematical and computational models is not well advanced.

Computational modelling of non-Newtonian flows, especially using Direct Numerical Simulation (DNS), shows promise in understanding transition and turbulence in these fluids. There have been some DNS of the turbulent flow of polymer solutions with an aim to understanding the causes of drag reduction ([1], [4], [10]). In all of these studies, very dilute polymer solutions were considered in which shear thinning behaviour was negligible and elongational effects were taken into account using various methods for the extra elastic stresses. For a wide range of important materials, the non-Newtonian rheology is primarily of a shear-thinning nature and there is very little in the literature on CFD modelling of turbulent shear-thinning non-Newtonian fluids without visco-elasticity.

This paper describes a study undertaken of shear-thinning non-Newtonian fluids whose rheology can be described using the Ostwald-de Waele or power law model, i.e.

$$\mu = K\dot{\gamma}^{n-1},$$

where K is the consistency and n is the flow index. Experimental results show that the transition to turbulence may occur more slowly than in Newtonian fluids and at higher (generalised) Reynolds number.

Experimental Method

The test facility consists of a fully instrumented mixing tank that feeds a special non-magnetic Warman International 4x3 centrifugal slurry pump. This pump feeds a 40m x 100mm-diameter pipe loop that passes through an MRI imaging facility

before it returns to the mixing tank. Flow can be diverted to a weigh tank for flow calibration and delivered density measurements. Optical windows are installed at the beginning and near the end of the loop. The MRI and second optical window are positioned at the downstream ends of the loop's straight sections to ensure that established flow conditions are examined. The rig is fully equipped with pressure and bulk flow transducers and is operated under computer control via a Labview SCADA system. A two colour TSI laser Doppler velocimeter (LDV) mounted on an industrial robot is used to measure the axial velocity profiles across the horizontal and vertical diameter of the pipe in the second optical window. Further details of this pipe test loop and associated instrumentation are given [8].

The fluid used in the present investigation was a 0.5 wt% aqueous solution of sodium carboxymethylcellulose (7HF Aqualon CMC supplied by A.C Hatrick). The CMC has a molecular weight of approximately 700 000 and is modelled as a power law fluid. The rheological parameters of the CMC were obtained using a Bohlin CVO50 constant stress rheometer as well as from analysis of the pressure drop versus bulk flow rate curve in the laminar flow regime in the pipe loop. Curve fits to the data yielded a range of parameter depending upon relatively subtle changes in temperature or shear history, examples of which are shown below where the Bohlin data is obtained using a cone and plate geometry. Rheological parameters based on the pipe data were used in the simulations.

	k	n
Bohlin	0.717	0.613
Pipe loop	0.506	0.686

Table 1: Rheology model parameters for 0.5 wt% CMC solution.

Numerical Method

The spatial discretisation employs a spectral element/Fourier formulation, which allows arbitrary geometry in the (x,y) plane, but requires periodicity in the z (out-of-plane) direction. The non-linear terms of the momentum equation are implemented in skew-symmetric form because this has been found to reduce aliasing errors. To allow a semi-implicit treatment of the viscous terms, the non-Newtonian viscosity is decomposed into a spatially-constant component, μ_r , and a spatially-varying component $\mu - \mu_r$. The spatially varying component is treated with a second-order explicit formulation and the constant component is treated implicitly, thus enhancing the overall numerical stability of the scheme (see [6] for details). The value of μ_r is chosen to be approximately equal to the maximum value of μ . This value is not known *a priori*, but can be adjusted during the computation without any adverse effects.

In order to drive the flow in the axial (z) direction, a body force equal to the pressure gradient measured in the experiments is applied to the z -momentum equation. This approach allows the pressure to be periodic in the axial direction.

The code runs in parallel using the message-passing kernel MPI, and the computations reported here were carried out using 8 processors on an NEC-SX5 supercomputer.

Validation

The underlying numerical code has been validated for both DNS and LES of pipe and channel flow (see for example [9]). The implementation of the power-law non-Newtonian viscosity was validated against laminar pipe flow and axisymmetric Taylor-Couette flow of power-law fluids, both of which have analytic solutions. In all cases, numerical results from the code agreed to within 0.01% of theory.

Computational Parameters

The computational domain consists of 105 8th-order elements in the pipe cross section (see Figure 1) and 96 Fourier modes in the axial direction ($3\pi D$ long). Numerical integration was continued until such time as the solution had become statistically steady. Averages were then taken over approximately 5 pipe-length traverse times. In terms of wall units, the near-wall mesh spacing is $r^+ \approx 0.5$, $R\theta^+ \approx 15$ and $z^+ \approx 30$. This resolution is marginal in the span-wise and stream-wise directions but sufficient for this preliminary investigation.

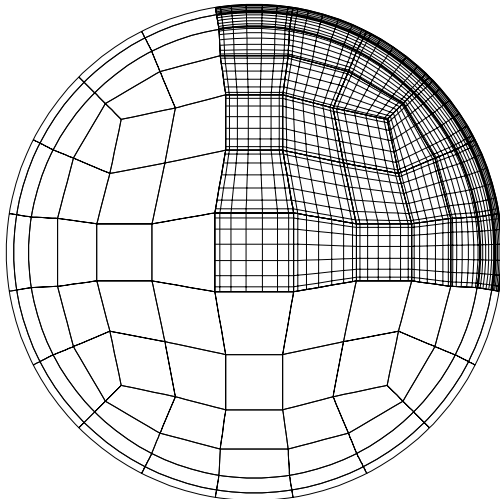


Figure 1 2-D cross-sectional mesh used for the DNS (the nodal mesh is shown in the upper right of the mesh only). A Fourier expansion with 96 modes was used in the axial direction.

Experimental Results

The transport characteristics of the CMC were measured (i.e. pressure drop as a function of superficial velocity) and it was observed that transition from laminar to turbulent flow was delayed and occurred at a generalised Reynolds number of approximately 3,500 (as opposed to approximately 2,300 for a Newtonian fluid or a power law fluid with $n=0.68$). The generalised Reynolds number is based on a wall viscosity that is determined from the mean wall shear stress. The wall shear stress is found from

$$\tau_w = \frac{D}{4} \frac{\partial P}{\partial z}.$$

Assuming a power-law rheology, it is then easy to show that

$$\mu_w = K^{1/n} \tau_w^{1-1/n}, \quad (1)$$

and this value is then used along with the bulk (or superficial) flow velocity and pipe diameter to define Re_G . This Reynolds number is different to the conventional K' and n' terms of the Metzner Reed approach.

The mean axial velocity profile for the CMC as measured by LDV is presented in Figure 2. For comparison, the DNS profile for a Newtonian flow at $Re=5,000$ and the $1/7^{\text{th}}$ power law profile (generally considered a good approximation at Re near 10^5) are included. From this data, it is difficult to distinguish the CMC results from the Newtonian results.

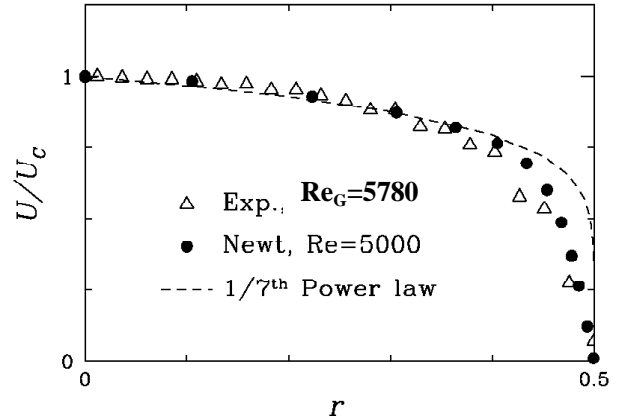


Figure 2 Experimentally measured velocity profiles for CMC compared to DNS results for a Newtonian fluid at $Re=5,000$ and the $1/7^{\text{th}}$ power law profile for reference.

Numerical Results

The results from two simulations are presented here. In Simulation 1, a pressure gradient equal to that measured experimentally is used. In Simulation 2, an increased pressure gradient is applied. When the pressure gradient used in the simulation is equivalent to that measured experimentally, a mean flow velocity of 0.73 times that of the experiment is predicted. When the pressure gradient is increased by 25% above the experimental value, the mean flow velocity increases, but only to 0.89 times the experimental value.

A number of different causes for this discrepancy have been investigated but only go part way to explaining the difference. Although LDV measurements of the flow had been taken, bulk flow velocities were estimated from a magnetic flow meter rather than being calculated from the LDV profiles. Despite careful calibration, the magnetic flow meter gave a velocity 12% higher than that estimated by integrating the measured LDV profile. This explains slightly less than half of the discrepancy between experiment and the Simulation 1 results and does not reduce the transitional Reynolds number to the expected value - the source of the difference between LDV and magnetic flow meter mean flow velocity estimates is yet to be resolved. Other factors that were considered, and subsequently ruled out, were 1) viscoelastic effects, 2) power law model parameters and 3) domain length effects.

1. It was estimated [2] that the highest shear rates in the turbulent boundary layer had time scales that were approximately two orders of magnitude too long for viscoelastic effects to be important.
2. Because the power law model for the CMC solution had been determined from shear rates less than approximately 500 sec^{-1} , and the peak values in the turbulent boundary layer were predicted to be of the order of 5000 sec^{-1} , the suitability of both the power law model parameters and the power law itself were called into question. In particular, the possibility of a high shear rate plateau (more appropriately modelled using a Cross viscosity model) modifying the high shear viscosities and hence the turbulent structures was a

possibility. Cross model parameter fitting from rheology data [2] suggested that the high shear plateau occurs for this material at significantly higher shear rates than those predicted here and is not likely to be a major source of error. The high shear viscosities predicted here are still several orders of magnitude higher than the carrier fluid (water) viscosity. It is still possible that the power law model parameters are having an influence and needs to be investigated further.

3. A final possible source of error is domain length effects. As seen in Figure 3, the near wall structures have lengths that are comparable to the domain length (especially for Simulation 1 at $Re=3964$). This will influence the results, although a similar simulation undertaken on a short domain of length πD resulted in an almost identical under-prediction of the mean velocity. Although domain length is an issue, it is not likely to be a major source of the error in mean flow velocity.

The wall streaks for both simulations show significant axial extent (Figure 3) especially for Simulation 1. The small disordered patches of red are more prevalent for Simulation 2 ($Re_G=5500$) and are suggestive of intermittency or bursting, and not of fully developed turbulence.

Velocity profiles in wall units are presented in Figure 4 for the experimental results, the two non-Newtonian CFD simulations and a DNS of turbulent pipe flow at $Re=5000$. The non-dimensionalisation is undertaken using the wall viscosity given in equation 1. The Newtonian profile is in good agreement with accepted profile for low-Reynolds number turbulent pipe flow (shown as the solid line). All profiles have a linear relationship between U^+ and y^+ in the near wall region. In the logarithmic region (where the flow is represented by $U^+ = A + B \ln y^+$), the experimentally measured profile for the CMC is very much above the low-Re Newtonian profile and has a totally different slope (B). This is consistent with results presented in [7] for various CMC solutions, where B increases with increasing CMC concentration (i.e. decreasing n). The experimental profile also has generally similar characteristics to a flow that is not fully developed.

The results for Simulation 1 ($Re_G=3964$) fall above the low-Re Newtonian profile but significantly below the experimentally measured profile. The results for Simulation 2 lie still closer to the Newtonian profile. As Re_G increases, the simulated results will approach the Newtonian profile, consistent with more developed turbulence as Re_G increases.

This approach to the Newtonian profile as Re_G increases is not consistent with the experimental results of [7] for CMC in which turbulence profiles for higher Re_G flows of CMC collapse onto a curve which has a value of B that increases with CMC concentration. More generally both A and B are usually considered to be inversely proportional to n [2]. For a concentration of 0.5 wt%, B is estimated to be approximately 25. However, the results are consistent with experimental results presented in [5] for turbulent flow of a well-sheared Laponite suspension (a synthetic clay that produces a thixotropic fluid). In those results, the profile for transitional flow appears very much like the experimental profile measured here for CMC. As Re_G increases, the value of A falls from around 8 and approaches the Newtonian value (albeit at much higher Reynolds numbers than simulated here). The value of B does not vary significantly from the Newtonian value once the flow becomes fully developed.

Turbulence intensities and Reynolds stresses are presented in Figure 5. From the experimental results, only azimuthal and axial turbulence intensities are available. The radial and azimuthal turbulence intensities are lower by 20-40% for the power law fluid simulations compared to the Newtonian DNS, whereas the axial intensities are marginally higher.

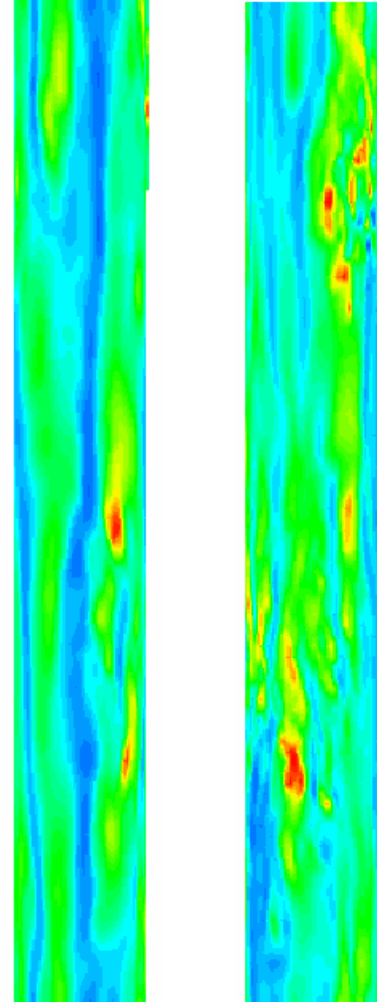


Figure 3 Near wall structure revealed in contours of streamwise velocity at $y^+=10$. $Re=3964$ (left) and $Re=5500$ (right). Near wall structures are very long, especially for the lower Reynolds number.

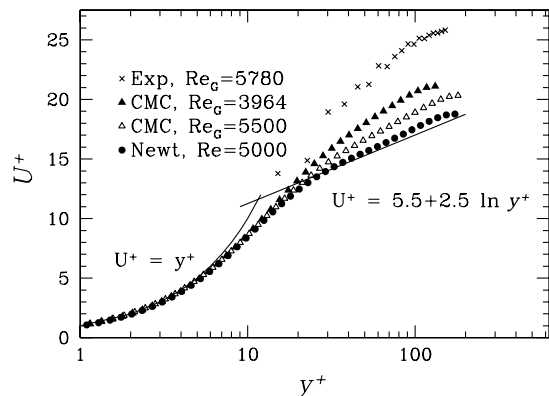


Figure 4 Velocity profiles in wall units for experimental and CFD results. The traditional law of the wall profile is also given with parameters suitable for low Reynolds number turbulence in a Newtonian fluid.

The experimental results also follow this trend which is in agreement with results presented in both [5] and [7]. The simulation results here suggest that as Re_G increases, the Newtonian profile will be approached, whereas the the results of both [5] and [7] suggest that the gap may not be breached.

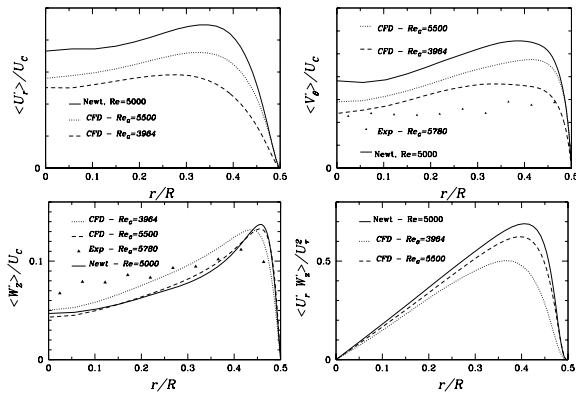


Figure 5 Turbulence intensities and Reynolds stress as a function of radius. Radial velocity (top left), azimuthal velocity (top right), axial velocity (lower left) and Reynolds stress (lower right). Symbols are for experiment, solid lines for Newtonian DNS and dashed and dotted lines for CMC simulations. As Re_G increases, CMC simulation results approach the Newtonian profiles.

Cross-sectional velocities for $Re_G=5500$ are shown in Figure 6 and show a qualitatively similar picture to low Reynolds number turbulence in a Newtonian fluid.

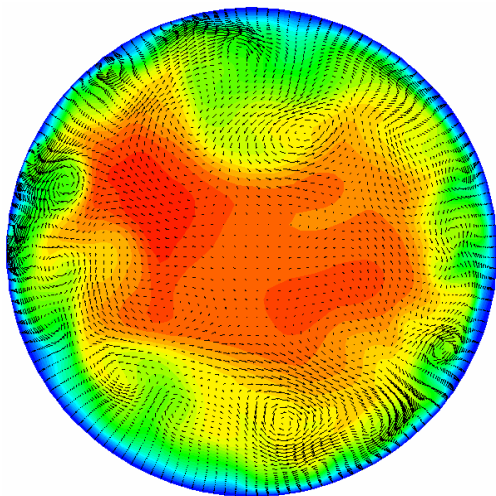


Figure 6 Contours of axial velocity and in-plane velocity vectors for $Re_G=5500$.

Discussion

The delayed onset of transition for this material suggests that the CMC solutions do not behave as simple power law fluids, and that rheological properties are present that cannot be modelled entirely by such a simple formulation. However it is certainly true that generally CMC is well described by this model, at least in the macro sense. The simulation results for a power law fluid show some agreement as well as some significant differences with the experimental results. Importantly there are significant quantitative differences between the simulation and experiment. The experimental measurements are in qualitative agreement with previously published experimental results for shear thinning thixotropic fluids [5] although differ qualitatively from results for CMC [7] and earlier works, e.g. [2] that have shown turbulent

profiles deviating from the Newtonian curves in inverse proportion to n . Careful attention was paid to validation of the numerical method both in turbulent Newtonian flow and in laminar flows of power-law fluids, and in both cases no errors were found. Although this does not rule out the possibility of fundamental error in the numerical method, it does not at this point appear to be a likely cause of the discrepancy between experiment and simulation. As discussed, part of the error in the mean flow velocity may be attributable to a calibration error and some additional (unknown) part may result from uncertainties in the power law model parameter fitting. This latter point will be considered in future simulation work. However, it is unlikely that either of these factors will in any way modify the nature of the mean flow profile as shown in Figure 4. It would appear that the simulation results have a different form to the experimental results for CMC that cannot be explained simply. The mean flow profiles have some qualitative agreement with experimental results for the shear thinning turbulent flow of Laponite [7]. However since the difference in flow behaviour between CMC and Laponite is partly due to their relative sensitivities to shear history, a feature not incorporated in this simulation, such agreement must at this stage be considered purely fortuitous. Another possible source of difference is the validity of the power law and generalised Newtonian fluid models for CMC solutions. Because the majority of shear rheometry is deliberately based on flows with a single component of shear, it may be that micro-structure develops in CMC solutions during rheometer measurement and the measured rheology is not applicable to a time-evolving, turbulent and three-dimensional flow field. If this were the case, it would suggest that an anisotropic viscosity that depends on the Lagrangian time history of a fluid element may be required to model so-called 'simple' fluids.

Acknowledgments

The authors acknowledge the support (via AMIRA project P599) of AMIRA, BHP, De Beers, Rio Tinto, Western Mining Corporation and Warman International in part sponsorship of this work.

References

- [1] Beris, A. N. and Dimitropoulos, C. D.. Pseudospectral simulation of turbulent viscoelastic channel flow, *Comput. Methods Appl. Mech. Engrg*, **180**, 365-392, 1999.
- [2] Bogue, R.L & Metzner, A.B., *Ind Eng. Chem. Fundam*, 2, 1963, p143
- [3] Chyrss, A., *Personal Communication*, 2001.
- [4] Dimitropoulos, C. D., Sureshkumar, R. and Beris, A. N.. Direct numerical simulation of viscoelastic turbulent channel flow exhibiting drag reduction: effect of the variation of rheological parameters, *J. Non-Newtonian, Fluid Mech.*, **79**, 433-468, 1998.
- [5] Escudier, M.P. and Presti, F. Pipe flow of a thixotropic liquid, *J. Non-Newtonian Fluid. Mech.* **62** 291-306, 1996.
- [6] Karniadakis, G.E., Israeli, M. and Orszag, S.A. High-Order Splitting Methods for the Incompressible Navier-Stokes Equations, *J. Comput Phys.* **97** 414-443 1991.
- [7] Pinho, F.T. and Whitelaw, J.H., Flow of non-Newtonian fluids in a pipe, *J. Non-Newtonian Fluid. Mech.* **34** 129-144, 1990.
- [8] Pullum, L. and L.J.W. Graham, A new high concentration pipeline test loop facility. in *Hydrotransport 14*. Maastricht, Netherlands 1999.
- [9] Rudman, M. and Blackburn, H.M., 'Large eddy simulation of turbulent pipe flow', 2nd International Conference on CFD in the Minerals and Process Industries, Melbourne Australia, 6-8 December 1999.
- [10] Sureshkumar, R., Beris, A. N. and Handler, R. A.. Direct numerical simulation of the turbulent channel flow of a polymer solution, *Physics Fluids*, **9**, 743-755, 1997.